FORMATION OF MULTIPLE-ASTEROID SYSTEMS

Eliot Halley Vrijmoet[1]

[1]*Georgia State University, Atlanta, GA 30302-4106*

ABSTRACT

Studies of multi-asteroid systems can yield fundamental information regarding their compositions and dynamics, allowing conclusions to be drawn addressing their formation and evolution. Because the processes involved in asteroid formation are shared with planet formation, the study of these systems has wide-reaching applications in the field of astronomy and in particular to the formation of our Solar System, as well as other planetary systems. In this work we consider the advances in asteroid surveys over the last ~40 years and the subsequent developments made in asteroid formation theory. This topic has shifted from location-specific scenarios to a unified model based on rotational physics and the Yarkovsky-O'Keefe-Radzievskii-Paddack (YORP) effect.

Keywords: minor planets, asteroids: general — planets and satellites: formation

vrijmoet@astro.gsu.edu

1. INTRODUCTION

Binary asteroids are systems composed of two gravitationally-bound asteroids. Similarly, triple asteroid systems contain three gravitationally-bound asteroids. These systems are commonly abbreviated as "binaries" and "triples," respectively. The primary component of a binary is usually the larger (in diameter) of the two bodies, with the smaller denoted as the secondary. We also note that these systems often have the secondary's rotation period synchronized to the orbital period, referred to as synchronous systems. A few are even doubly-synchronized: both the primary and secondary share a rotation period that matches their orbital period. Systems in which no synchronization occurs are referred to as asynchronous.

Multi-asteroid systems are common: for example, nearly 15% of near-Earth asteroids with diameters greater than 200 m are in multi-asteroid systems, and the fraction in the main belt is expected to be similar (Margot et al. 2002; Pravec et al. 2006). The additional information yielded by the dynamics of these systems allows the determination of asteroid characteristics that are otherwise more opaque, e.g., total system mass for the two asteroids, density, and mass distribution. From these properties we can derive insight into potential composition of the asteroids without resorting to more expensive or limited means such as spacecraft flybys. We can also derive detailed characteristics for a set of representative objects that potentially span a wide range of physical space and photometric properties; these inferences can then be applied to much larger populations.

A significant set of asteroid compositions, mass distributions, orbital characteristics, and other properties provides a statistical picture of the situation complete enough to constrain the formation and evolution of these objects. The processes involved in the formation of these small, rocky bodies are fundamentally similar (if not identical) to those that contribute to the formation of their larger cousins, the major planets. Thus, understanding the nature of mass accretion, tidal forces, collisional processes, etc., through the easily-available lens of asteroids provides valuable insight into the more data-starved realm of planet formation.

A single asteroid's *size* is a tricky concept, considering the irregular shapes of most of these objects. In this paper, we quote the asteroid diameter as its size, except in those cases where we specify its length along the three axes of the ellipsoid that best approximates it. Because the fundamental properties of multiple-asteroid systems depend most strongly on the constituent asteroids' sizes, it is essential to make clear the different asteroid populations defined in the Solar System, given that the distributions of asteroid sizes also depends strongly on the population being considered.

Near-Earth asteroids (NEAs) are asteroids with orbits that take them within 1.3 AU of the Sun at perihelion (checked in De Pater & Lissauer). As of 2017 April 25, there are 16,058 of these asteroids listed at the *Minor Planet Center*[1]; their current locations are shown as red circles in Figure 1. The vast majority lie between the orbits of Mars and Mercury. Binary NEAs are small, with primary components of known systems not exceeding 10 km in diameter and secondaries $4-58\%$ the size of their primaries (Walsh & Jacobson 2015).

Main belt asteroids (MBAs) reside between the orbital paths of Mars and Jupiter; they appear as the green circles in Figure 1. The sizes of binaries in this population vary more widely than for the NEAs, from less than 1 km to hundreds of km (Warner et al. 2009).

Trans-Neptunian objects (TNOs) are located outside the orbit of Neptune. For space reasons, we will not consider them in this work. A suitable introduction can be found in the review by Richardson & Walsh (2006). For similar reasons, we will also omit discussion of Jupiter Trojans.

---

[1] Available online at `http://www.minorplanetcenter.net`

Early surveys for multi-asteroid systems were limited primarily by the resolution of their instruments, hence the first binary asteroids discovered were larger main belt objects rather than those smaller objects in the closer near-Earth population. In this paper we focus on NEAs and MBAs; Sections 3 and 4 discuss the early searches in these areas and their location-specific results. Early formation mechanism theories were (and continue to be) influenced heavily by these results that are biased toward location, but as the diversity of known multi-asteroid systems increased, so too did our understanding of formation as a strong function of size. Section 4.3 outlines the more recent observational developments, and Section 5 discusses the resulting current understanding of binary asteroid formation mechanisms in depth. In Section 6 we present and discuss a compilation of all known binary NEAs and MBAs through March 2016.

2. PERSONAL MOTIVATION

The reason I initially chose to study physics was quantum mechanics, but my ultimate motivation for staying in the field was classical mechanics. Quantum mechanics became more mysterious and less satisfying as we learned more about it—despite (in retrospect) admirable attempts by our professors to demonstrate its simultaneous power and simplicity, it seemed to be a black box with interesting mathematics but physical explanations that bordered on mysticism. Classical mechanics, however, revealed itself to be physics' redeeming factor. Nearly every situation was intuitive and could be reduced to a set of Euler-Lagrange equations which were solvable with interesting mechanics but no *deux ex machina* leaps of logic. Classical mechanics is the hero of physics.

Astronomy was appealing because it fundamentally relied on classical mechanics acting in the pristine environment of outer space. It soon became apparent that the majority of space objects required an alarming amount of atomic physics to be properly understood, but one could ease into the situation by considering the many geometrical situations in depth before tackling spectroscopy.

That interest in classical mechanics and interesting geometry led me to binary stars and exoplanets. These topics were consolation prizes, as they were not so clean as my imagined billiard balls in space, but time bred familiarity and appreciation for them. When considering planetary sciences, however, I discovered that the old dream could finally be realized: asteroids are simple, rocky structures, and some of them appear in interesting gravitational situations. Better yet, the consequences of their compositional variations add just enough spice to their studies. I am finally ready to acknowledge that pure, homogeneous billiard balls in space would become tedious and predictable a little too quickly.

Binary asteroids are thus interesting because they are relatively simple in structure (compared to, for example, stars) and engage in a wide variety of geometrical and dynamical situations. Their formation is interesting because it (currently) seems to depend on the dynamical situation more than composition and temperature. The history of the study of this topic follows the typical astronomy narrative of more unusual systems being the first discoveries or discovered in the more unusual ways, and the shifts in understanding that followed over the next 40 years were varied and imaginative.

3. EARLY SEARCH PROGRAMS

The possibility of asteroid companions was considered as early as 1901, when the light curve of Eros was noted to have variations similar to eclipsing binary stars (a summary of this history can be found in Merline et al. 2002a). The idea was compelling enough to inspire numerous concentrated efforts through the mid-1970s and 1980s, but these searches discovered only indirect evidence (such as reports of asteroids briefly occulting stars) that could not be convincingly differentiated from instrumental or atmospheric effects at that time. The first binary asteroid was not discovered until the *Galileo* spacecraft imaged (243) Ida and its

companion Dactyl. This section discusses those earliest, pre-Ida efforts and the limitations that contributed to their lack of success.

3.1. *Methods and Results of the Earliest Searches*

Direct imaging, which ultimately provided the earliest confirmed evidence of binary asteroid systems, was initially unsuccessful due to lack of adequate angular resolution and dynamic range. Asteroid companions are typically separated from the primary component by much less than one arcsecond and are many magnitudes dimmer; for example, the companion to (762) Pulcova, one of the first objects found with direct imaging, is about 4 magnitudes fainter than its primary and is separated by 0.6″ on the sky (Merline et al. 2000b). Merline et al. (2002a) also give the example that a 50-km asteroid in the Main Belt (at 2.5 AU) would appear separated from a 2-km companion by as little as 0.02 to several arcseconds and as many as 7 magnitudes in brightness. Early imaging searches such as Gehrels et al. (1987) and Gradie & Flynn (1988) were limited to minimum separations of about 2 arcseconds at best and rarely searched more than 30 targets.

Anomalous light curves at the time were also suspected to belong to binary asteroid systems. These light curves had slopes that suggested eclipse events, specific shapes/flatness at times of minimum light, and fluxes that depended strongly on phase angle. Figure 2 illustrates the light curve of (39) Laetitia from Cellino et al. (1985), who selected 10 similar light curves of Main Belt objects for modeling with a pair of triaxial ellipsoids with varying mass ratios. Light curve analysis consistently failed to produce unique solutions to any system, thus its results were considered interesting but far from definitive evidence.

3.2. *Formation Mechanisms Proposed Based on Early Results*

With the lack of empirical results from surveys, early formation theories for binary asteroids were poorly constrained and varied greatly based on the assumptions taken by the numerical models at that time. The triaxial ellipsoidal models of Leone et al. (1984) were groundbreaking because, unlike previous attempts, they do not assume spherical asteroids—the consideration of possibly "irregular" shapes are a side note rather than a *requirement* of the model for even that author. Considering mass ratios ($q = M_S/M_P$) smaller than 1.0 is another novelty of that work.

The prevailing theories for binary asteroid formation in this era centered on collisions as the event triggering multiplicity. The "rubble-pile" structure of asteroids was viewed as a reasonable assumption (and has since been commonly accepted), thus one reasonable scenario was rotational fission following transfer of angular momentum during a collision—an idea that has persisted to this day (see Section 5 of this work). Also popular was the idea that ejecta or debris following a collision may become trapped in the gravitational field of an asteroid and thus form a companion body.

For example, Gehrels et al. (1987) used the likelihood of the trapped-ejecta scenario to support their own lack of results by asserting that the smaller sizes of asteroids (compared to, e.g., terrestrial planets) reduces the range of velocities required for debris to orbit without reaching escape velocity or falling onto the asteroid surface. They note that the asteroid masses reduce this possiblity to the point that enough debris reaching this "goldilocks zone" to form an asteroid companion is extremely unlikely. They argue further that any satellites must be formed during the time when the solar nebula was still dense enough to slow an asteroid's motion through space, increasing the likelihood of accumulation and/or capture. Davis et al. (1985) found that satellites smaller than 30 km in diameter would be too easily perturbed out of their orbits via collisions with other objects to survive from the time of asteroid formation until now. Because objects 30 km or greater at asteroidal distances should be visible with the instrumentation of the late 1980s, Gehrels et al. (1987) concluded that their lack of results is indicative of a true lack of asteroid companions.

4. SUCCESSES AND SUBSEQUENT SEARCHES

4.1. *Earliest Successes with Main Belt Asteroids (MBAs)*

In 1993 the satellite Dactyl became the first confirmatory evidence of a companion orbiting an asteroid—in this case, around 243 Ida (Chapman et al. 1995). Dactyl was imaged by the *Galileo* spacecraft in a set of 47 images (taken at 18 different times) over a period of 5.39 hours, and through these data and subsequent modeling was shown to have mean radius of 0.7 km, or about 4% of that of Ida (15.7 km) (Belton et al. 1995). Reflectance spectra of Dactyl and Ida suggest that they formed from the same asteroid family (Koronis), although they do show evidence of different amounts of space weathering. Considering this information together with its small size, it was concluded that Dactyl was not a captured previously-heliocentrically-orbiting object, but formed from either Ida itself (e.g., from ejecta from a large impact on Ida) or from the same collision event that created the Koronis asteroid family. The latter explanation was favored primarily due to Ida's high crater density, which suggests a local small-body collision rate too high to support the formation of Dactyl in its currently stable orbit.

Dactyl's discovery was followed up with numerical models that pointed toward such collision-created binary scenarios being common, described by Durda (1996) as "a natural outcome of catastrophic collisions" and able to generate configurations with a range of morphological type (contact vs. non-contact) and size ratios (large-tiny pairs vs. equal-size pairs). Spurred by such results and aided by the late-1990s rise in adaptive optics, in 1999 a ground-based search for asteroid companions of 200 objects discovered a moon orbiting 45 Eugenia (Merline et al. 1999a). This object, designated S/1998 (45) 1 and later named Petit-Prince, was estimated to have a diameter of 13 ± 3 km, or about 6% of Eugenia's 215 ± 4 km (Merline et al. 1999b). That size ratio and the non-sphericity of Eugenia suggested a collisional formation scenario for the pair, likely with the satellite forming from ejecta of a large impact on Eugenia.

Additionally, the density of (45) Eugenia derived from the orbit of Petit-Prince was surprisingly low at about 1.2 g cm^{-3} despite its categorization as an FC-type, suggesting a significant rubble-pile interior. This result was supported by the similar findings regarding (253) Mathilde, a C-type, which spacecraft flyby found to have 1.3 g cm^{-3} Veverka et al. (1999).

Although the discovery of S/1998(45)1 served to demonstrate that Dactyl was not a unique object, the authors of that study remained convinced that large-small pairs were uncommon. Flybys of *Galileo* and the Near-Earth Asteroid Rendezvous (NEAR) probe had failed to find evidence of satellites around 253 Mathilde (Merline et al. 1998), 433 Eros (Merline et al. 1999c; Veverka et al. 1999), nor the (somewhat smaller) 951 Gaspra (Belton et al. 1992), despite unprecedentedly thorough searching of these objects' spheres of gravitational influence. Somewhat earlier ground-based studies (Gehrels et al. 1987; Gradie & Flynn 1988) and an HST search (Storrs et al. 1999) had likewise failed to find evidence of asteroid satellites, providing a growing lack of evidence to counter the increasing numerical suggestions that large-small pairs could form long-term stable orbits with relatively high frequency.

Nonetheless, additional MBA binaries followed Petit-Prince and (45) Eugenia in the early 2000s, e.g., (90) Antiope, (762) Pulcova, (87) Sylvia, (3749) Balam (Merline et al. 2002b), and (121) Hermione (Merline et al. 2002c).

4.2. *Discoveries of companions of Near-Earth asteroids (NEAs)*

Asteroid companions for the near-Earth population were first suggested as the cause of "doublet craters," (Melosh & Stansberry 1991; Bottke & Melosh 1996), or large (> 20 km diameter) craters on Earth with ages that indicate the simultaneous creation of both components. Additional evidence for near-Earth binary

asteroids was spotted in light curves (Pravec & Hahn 1997; Pravec & Harris 2000) that exhibited two distinct rotation periods and eclipses and occultations of the primary object. Neither of these observations (doublet craters and anomalous light curves) were enough to bring the existence of near-Earth binaries to the point of "universal acceptance" until radar images revealed 2000 DP107 (at 1.37 AU) and four other NEAs to have binary companions (Margot et al. 2002, and references therein).

Radar is an attractive tool for studying near-Earth asteroid binaries because it provides both spatial and frequency (Doppler) information of the target. Frequency information can produce a characteristic super-imposed double peak in the echo power spectrum (see Figure 3). At radar wavelengths it is reasonable to achieve angular resolution better than 1 milliarcsecond and to collect data on a full orbit of the secondary around the primary. These advantages make it an excellent tool for forming a complete quantitative under-standing of the binary scenario.

The five NEA binaries announced in 2002 allowed estimates of binary prevalence that drew a stark line between this population and the MBA binaries: Margot et al. (2002) stated that as many as 16% of NEAs greater than 200 m in diameter were binary systems, compared with roughly 2% for MBAs. These figures agreed with simulations and light curve studies. They attributed the difference in prevalence to the NEAs' more frequent interactions with the inner Solar System planets.

The spin rates of the binary NEAs were too high ($P_{\rm rot} \approx 3$ hours) to support the impact-driven formation scenarios that had explained the MBA binaries. Although it was possible that they could spin up so high from transfer of angular momentum during a collision, these shorter spin periods were not a *necessary* outcome of most collisions; it was just as possible for collisions to produce longer spin periods. Those formation theories also predicted larger size ratios to be more common among the pairs than were suggested by the radar observations. The most compelling explanation for these objects was rotational fission, a scenario involving mass loss as a result of an impact and subsequently high spin rate on a strengthless body. The details of this theory are expanded in Section 5 of this paper.

4.3. *Recent Observational Improvements and Successes*

In the past 15 years the number of known binary asteroids has improved to the point where the binary NEAs have increased more than fourfold and the binary MBAs have more than doubled. Johnston (2016) reports 282 binary systems in the Solar System as of 2016 March 31, including far objects such as TNOs and Jupiter Trojans. These successes have been driven by improvements in instrumentation and have fueled vast improvements in our ability to accurately model these systems' formation and evolution in numerical simulations.

In particular, new techniques are becoming viable that were impossible in the early days of binary asteroid surveys. One notable example is stellar occultation, in which the dimensions of an asteroid companion can be inferred from the chord of an asteroid's path across the face of a star. Successful implementation of this technique requires simultaneous observations of the occultation from multiple positions on the Earth, thus it is quite sensitive to the accuracy and precision of the pre-established ephemeris of the asteroid expected to do the occultation. Well-constrained, reliable asteroid ephemerides, ability to accurately synchronize obser-vations, and simultaneous availability of multiple observatories are essential factors for this technique that have benefited greatly from the technological improvements of recent years (e.g., with Global Positioning System or GPS).

In 2002, Merline et al. (2002a) assert that although the rate of NEA binaries has been shown to be 15% and many MBA satellites have been identified, the rate of binarity among MBAs must be not much higher than about 2%. Eleven years later, in an updated review, Margot et al. (2015) claim that the photometric discovery

rate of binary MBAs has been so high that they are likely as prevalent as binary NEAs. No quantitative estimate is made at that time because the observational selection effects are not yet well-described and accounted for.

5. FORMATION THEORIES

Among the NEAs and MBAs, likely formation scenarios for multi-asteroid systems may be considered based on the size of the primary asteroid. A primary diameter (D_P) of about 20 km seems to be the greatest size at which an asteroid would be affected by the Yarkovsky-O'Keefe-Radzievskii-Paddock (YORP) effect substantially enough to drive the formation of a companion (secondary). Hence, we choose that size as the dividing line between "small" ($D_P < 20$ km) and "large" ($D_P > 20$ km) systems in the discussion below.

5.1. *A Note Regarding Mutual-capture Formation Scenarios*

In the sections below we omit discussion of mutual-capture theories because it is unlikely that such scenarios play a significant role in the creation of multi-asteroid systems among the NEAs and MBAs. Mutual capture requires that two or more pre-existing asteroids pass within each other's gravitational spheres of influence at speeds slower than their escape velocities, resulting in a gravitationally bound system. The NEAs and MBAs pass each other much too quickly to enable capture; their encounter speeds (the speeds at which they pass near each other) are on the order of km s^{-1}, whereas their escape velocities are on the order of m s^{-1} (Richardson & Walsh 2006, and references therein). This situation would be alleviated somewhat in the early Solar System, when the density of planetesimals was much higher, but only among the TNOs do we expect the dynamical situation (collisional lifetime) to enable these primordial multi-asteroid systems to persist until today (see, for example, Petit & Mousis 2004).

5.2. *Formation of Small Multi-Asteroid Systems ($D_P < 20$ km)*

For small asteroids, multi-body formation relies significantly on rapid rotation and subsequent "rotational fission" of ejecta into companion asteroids. Substantial work regarding this scenario was done by Weidenschilling (1980a,1980b), who considered the physical implications of these rapidly rotating bodies before modern surveys made high-quality empirical data available. Rotational fission considers that all bodies with no shear or tensile strength (so-called "strengthless" bodies) have a critical spin rate ω_d at which the centrifugal force exactly matches the gravitational force (and any other forces, such as molecular for very small asteroids) holding the body together. This critical rate is often quoted in terms of the body's mass density ρ and the universal gravitational constant G as $\omega_d = \sqrt{4\pi\rho G/3}$. Attempts to exceed this critical spin rate instead result in ejection of mass from the system.

Super-critical asteroid rotation results in mass migrating from the poles to the equator of the body in addition to ejection of the asteroid's mass from the equatorial region. The asteroid then takes on a distinctive top shape with an equatorial bulge, as modeled for 1999 KW4 by Ostro et al. (2006) (see Figure 4). The ejecta orbit the primary and coalesce into the secondary asteroid.

The spin-up of the primary asteroid to a super-critical, mass-shedding state may be triggered by the transfer of angular momentum from a sub-catastrophic collision, as was posited for 1999 KW4 (Margot et al. 2002). For small asteroids (diameter < 20 km), however, the driving force is likely the Yarkovsky-O'Keefe-Radzievskii-Paddock (YORP) effect.

The YORP effect is an extension of the Yarkovsky effect (for a detailed description, see Section 2 of Bottke et al. 2002, and references therein), which states that objects with sizes between 0.1 and 20 km lose angular momentum when they absorb photons from the Sun and reradiate these photons (typically at infrared

wavelengths). Consider an asteroid in heliocentric orbit. Incident photons from the Sun heat the asteroid, and in accordance with Kirchhoff's laws the heated asteroid radiates energy in the form of photons, which each carry away some momentum depending on their energies modified by the speed of light ($p = E/c$). The hottest part of the asteroid radiates the most photons, resulting in a "radiation recoil" effect that pushes it in the direction opposite its hottest surface. Because the asteroid has some pre-existing spin and some thermal inertia, its hottest surface is not directly facing the Sun but is instead within the quadrant between 0 (directly facing) and $\pi/2$ (one quarter turn) radians in the direction of its individual spin. The result is a net force directed partially radially outward (away from the Sun) and partially azimuthally (parallel to a heliocentric circular orbit). Depending on the existing orbital and physical properties of the asteroid, its orbital semi-major axis would then increase or decrease (in-spiral; if orbiting retrograde) in a significant matter over the course of several orbits.

A variation of the Yarkovsky effect is the YORP effect, which relies on the same principle of reradiated photons carrying away angular momentum, but creates changes in the object's spin rate rather than its orbital motion. As in the Yarkovsky effect, incident sunlight heats the asteroid's surface, which then reradiates this energy as momentum-carrying photons. For an object with an asymmetric surface as projected in the plane of the sky from the Sun's perspective (i.e., as projected in the plane perpendicular to, and along, the line of sight between the object and the Sun), photons are not radiated evenly across the object's surface even in the post-Sun quadrant discussed above, resulting in a net torque on the object. This torque, if acting in the direction as the existing spin, increases the spin rate of the object (Rubincam 2000). This effect may occur on relatively short timescales; for example, Bottke et al. (2002) state that the asteroid (951) Gaspra (radius 6 km, semi-major axis 2.21 AU) would take 240 million years to experience a rotation period decrease from 12 hours to 6 hours. The timescale is sensitively dependent on asteroid size, however, as Phobos (radius 11.1 km, orbiting Mars about 1.5 AU from the Sun) would experience such changes on a timescale of several billions of years. Hence, the dividing line above which we expect little noticeable spin effects from YORP is set at an asteroid diameter of 20 km.

Including the YORP effect in numerical models successfully reproduces the observed distribution of spin rates among small asteroids (Pravec et al. 2008; Rossi et al. 2009). These asteroids' spin periods had been shown to be inconsistent (both too low and too high) with the Maxwellian distribution that would be produced for a collision-dominated evolution. The confirmation of YORP as a dominating driver of asteroid spins also refuted the claim that spin rate distributions were location-dependent (Polishook & Brosch 2009).

The YORP effect has been shown to be a convincing mechanism for asteroid spin-up and resulting rotational fission. In a compilation of all observed binaries among the NEAs, Mars-crossing asteroids (MCAs), MBAs, and Jupiter Trojans, Pravec & Harris (2007) find that binaries with $D_P \leq 10$ km have spin periods very near to the critical limit. Their plot of primary diameter vs. primary spin period, reproduced here in Figure 5, shows that this near-critical spin is observed consistently for the binary NEAs and small MBAs and MCAs (group A in their plot) with small companions ($D_S/D_P \leq 0.5$). The MBAs and MCAs in Group A tend to be asynchronous, with the secondary asteroid's spin rate unconnected to (unsynchronized with) its orbital period about the primary. Group B contains small systems ($D_P \leq 10$ km) with components of near-equal size (D_S/D_P close to 1); these cases show synchronous rotation of the secondary, i.e., its spin period matches its orbital period (to borrow a term from another subfield, it is "tidally locked"). Group L systems are large and are addressed in our work in Subsection 5.3.

The secondary asteroids formed from YORP-induced rotational fission may be comparable in size to the primary, but smaller secondaries are observed more frequently. Pravec & Harris (2007) suggest that these

groups are not the results of two distinct sets of initial conditions or evolutionary paths, but rather reflect diversity among a single population. The transfer of mass from the primary to the secondary may be an extended process rather than a single short-term event, described by Pravec & Harris (2007) as involving the secondary continuously lifting matter from the primary's surface to its own surface via tidal attraction as it orbits. This process would continuously transfer torque from the primary to the secondary, slowing the primary's rotation and increasing the secondary's orbital semi-major axis. The observed size (and mass) ratio would then be a reflection of the time elapsed since critical spin was achieved (barring any complicating events perturbing the system during mass transfer, such as the close passing of a third body). Thus, the groups A and B in Figure 5 would be two ends of the same population.

5.2.1. *Evolution of Small Binary and Multi-Asteroid Systems*

Evolution once rotational fission has created a companion to the primary proceeds in a matter that depends on the mass ratio of the system. This process is summarized in Figure 6, reproduced from Jacobson & Scheeres (2011). The system created from the YORP mechanism is initially chaotic and binary.

For high mass ratio systems ($q = M_S/M_P > 0.2$), the two components tend to synchronize on tidal timescales (approximately $10^4 - 10^6$ years) to form a doubly synchronous binary. This system would have both the primary and secondary synchronized with its orbital period such that the two components constantly see the same side of each other (always face each other). Over sometimes longer timescales ($10^5 - 10^6$ years), the YORP process would act on the secondary component in what is called binary YORP, or BYORP.

BYORP, proposed in the seminal paper by Ćuk & Burns (2005) (and summarized succinctly in Vokrouhlický et al. 2015), states that an asymmetrical secondary asteroid synchronously orbiting its primary would feel a net force (from YORP) that causes its orbital separation to increase or decrease (spiral in). The eventual result of this situation for a doubly synchronous binary system with high mass ratio would be a contact binary (both components touching each other) in the case of in-spiral. If BYORP increases the orbital separation, then the two components would eventually cease to be gravitationally bound and would form an asteroid pair (two that are genetically related and on similar heliocentric orbits but are not orbiting each other).

For low mass ratio systems ($q = M_S/M_P < 0.2$), the initially chaotic binary may quickly (on dynamical timescales less than 1 year) become disrupted and form an asteroid pair. In other cases, the spin-orbit coupling can spin up the secondary until it undergoes rotational fission, ejecting mass that may return to the primary, escape the system entirely, or accrete into a third component of the system. In the former two cases, the ultimate outcome may be an asteroid pair, a stable binary system, or a single reshaped asteroid (loss of the secondary component).

A binary that remains after this process of secondary mass loss may experience secondary synchronization due to tides and subsequently would evolve via the BYORP effect as for the high mass ratio scenario described above.

A triple system created from rotational fission of the secondary could stabilize via tidal processes and become a system that we can observe today. There are also a few triple systems in which the third component may have formed from a second round of rotational fission of the primary, such as the NEA (153591) 2001 SN263 (Becker et al. 2008; Nolan et al. 2008; Delbo et al. 2011).

5.3. *Formation of Large Binary Asteroids ($D_P > 20$ km)*

The primary components of large binary asteroid systems spin faster than the average rates for similarly-sized single asteroids, but not fast enough to trigger rotational fission; see Group L in Figure 5. Numerical

simulations such as Durda et al. (2004) have shown that the observed companions of large asteroids may be created via collisions with 10- to 30-km objects at encounter speeds of 3 km s^{-1} to 7 km s^{-1}. As discussed in the beginning of Section 5 of this work, these speeds are reasonable for the NEA and MBA populations.

In nearly all cases, the mass ratios for large binary systems are between 10^{-6} and 10^{-2}. The secondary components for the smaller q systems are likely composed of debris from the aforementioned impact of the 10- to 30-km object with the parent body. If the impact is catastrophic, however, the parent body may split into two slightly more equally-sized components, creating q values closer to the 10^{-2} limit.

The case of (90) Antiope remains an outlier to the above scenarios, as it contains a primary with diameter 91 km and a nearly equally-sized large secondary with 86 km (Descamps et al. 2007). This system is apparent in Figure 5 as the point in the upper right corner of the "double, synchronous" box enclosing Group B. Pravec & Harris (2007) note that its angular momentum is near to same critical range of values that the small asteroid groups A and B cluster around, possibly implying some rotational fission process, but they assert that more data are needed to draw convincing conclusions regarding this property. Descamps et al. (2007) also suggest a rotational fission scenario following an oblique, sub-catastrophic impact on an already fast-rotating parent body. Analysis of light curve anomalies of the system in 2009 supported this scenario; given the number and size distribution of projectiles in the family containing (90) Antiope (Themis), they find that the probability of a family member creating such an impact event with an Antiope parent is greater than 50% over the lifetime of that family.

6. DISCUSSION

6.1. *Compilation of Multi-Asteroid Systems*

Johnston (2016) maintains a database of all binary asteroid systems in the Solar System and their fundamental known parameters. To illustrate the trends discussed in the above sections, we have collected a subset of this database composed of only the NEAs and MBAs (208 systems out of the 282 in the original full set). This means we omitted from the sample Johnston's categories of Mars Trojans, Jupiter Trojans, plutinos, Cubewanos, scattered-disk objects, Neptune-resonance objects, and other TNOs. Our subset is tabulated in Table 1 along with a few parameters of interest. Not all of the entries have values defined for our parameters of interest; missing values are indicated by "N/A." References for those values are too numerous to list here; they may be found at `http://www.astro.gsu.edu/~vrijmoet/asteroidrefs.html`.

Figures 7 through 10 illustrate those parameters of interest using a set of histograms, displayed for the entire data set of Table 1 as well as separated by Solar System location.

The densities in Figure 8 cluster around 1.6 g cm^{-3}, typical for most asteroids. The distribution is roughly the same for both MBAs and NEAs, suggesting similar origins.

The distribution of primary diameters D_P in Figure 9 is broader and centered around a larger value for the Main Belt asteroids than for the near-Earth asteroids. The NEAs are subject to more frequent gravitational perturbations (and subsequent loss of one or both binary components) than the MBAs due to their proximity to the inner Solar System planets, thus their tendency toward smaller sizes is not surprising. We must also consider the selection effect that is inevitably affecting this comparison: small NEAs are more easily detected by Earth-based observations than small MBAs, so it is possible that a large fraction of the existing small MBAs are missing from the distributions here. This effect is currently difficult to characterize and quantify without additional data from the Main Belt. Numerical simulations could estimate the expected distribution of asteroid sizes, but these models are currently informed by educated estimations

rather than empirical results—our nearest large asteroid population has the complicating factor of many more heliocentric orbiting planets than in the Main Belt.

The rotation periods of the primary asteroids are plotted in Figure 10. As discussed above (see Section 5 and Figure 5), the clustering around spin periods of about 4 hours is expected from a YORP-induced rotational fission model.

Figure 7 shows the size ratios D_S/D_P clustering around 0.25 for the whole set, with a smaller spike much closer to 0.0. The population-split histogram reveals that that secondary peak is probably due to the MBAs, as the NEAs are distributed slightly more evenly and mostly clustered at ratios just above 0.2. Assuming identical densities for each binary set (common practice in this field and shown to be reasonable for asteroid binaries), these results indicate mass ratios clustered around $q = 0.016$ for the largest MBA peak, the smaller MBA peak around 10^{-3}, and the NEA peak around 0.008. If a larger primary asteroid diameter makes companion formation via rotational fission less likely and formation via collisions more likely, then Figure 7 together with the primary-diameter distribution in Figure 9 and the rotational-period distribution in Figure 10 could support the speculation of Pravec & Harris (2007) that the tidal evolution timescale of asteroid binaries is inversely proportional to the primary asteroid's size. This would mean that the larger binaries are simply more tidally evolved versions of the smaller binaries.

6.2. *Summary and Conclusions*

We have discussed how the evolution of small binary asteroids (and non-binary asteroid pairs, or those that are genetically related but not bound gravitationally) varies based on their mass ratios and is tied to their spin rates and the YORP effect. Asteroids that rotate at the critical spin rate undergo rotational fission, forming companion asteroids from their own ejecta. The YORP effect is the driver of such spin-ups for asteroids smaller than about 20 km, but larger asteroids may be spun up following well-placed sub-catastrophic collisions with other bodies (transfer of angular momentum).

More commonly, however, the spin rates and angular momenta of large binary asteroids are insufficient for rotational fission, suggesting a somewhat different evolution path than that of the small binaries. Their mass ratios suggest that their secondary components formed via collisions between the primary component and other asteroids.

Formation and evolution of multi-asteroid systems has been narrowed down to a unified dynamical picture based on rotational physics and subsequent effects based on object sizes and mass ratios. This paradigm supersedes the earlier models that were strongly influenced by observational biases inherent to surveys of those eras, and is well-supported by modern numerical simulations. Although current instrumental techniques cannot completely eliminate such biases, especially considering the small sizes of most asteroids, this situation will improve with upcoming improvements in instrumentation.

In particular, we anticipate great things from the advent of 30-meter class telescopes such as the Thirty Meter Telescope (TMT) and European Extremely Large Telescope (E-ELT), as such instruments could resolve smaller separations between objects as well as better constrain the parameters of those systems already known. Improved precision for asteroid ephemerides, for example, would allow the technique of stellar occultation to be a more fruitful, less risky option for discovering and characterizing asteroid companions. There are also two space missions planned with the intent to collect samples and return to Earth: NASA's Origins Spectral Interpretation Resource Identification and Security-Regolith Explorer (OSIRIS-REx) and the Japan Aerospace Exploration Agency's Hayabusa-2 (already launched in December 2014). Efforts such as these will produce uncountable amounts of new information regarding their targets,

as they will have all the gravitational adventures of a typical flyby while also returning physical evidence of their target asteroids' surfaces.

Plot prepared by the Minor Planet Center (2017 Apr.25)
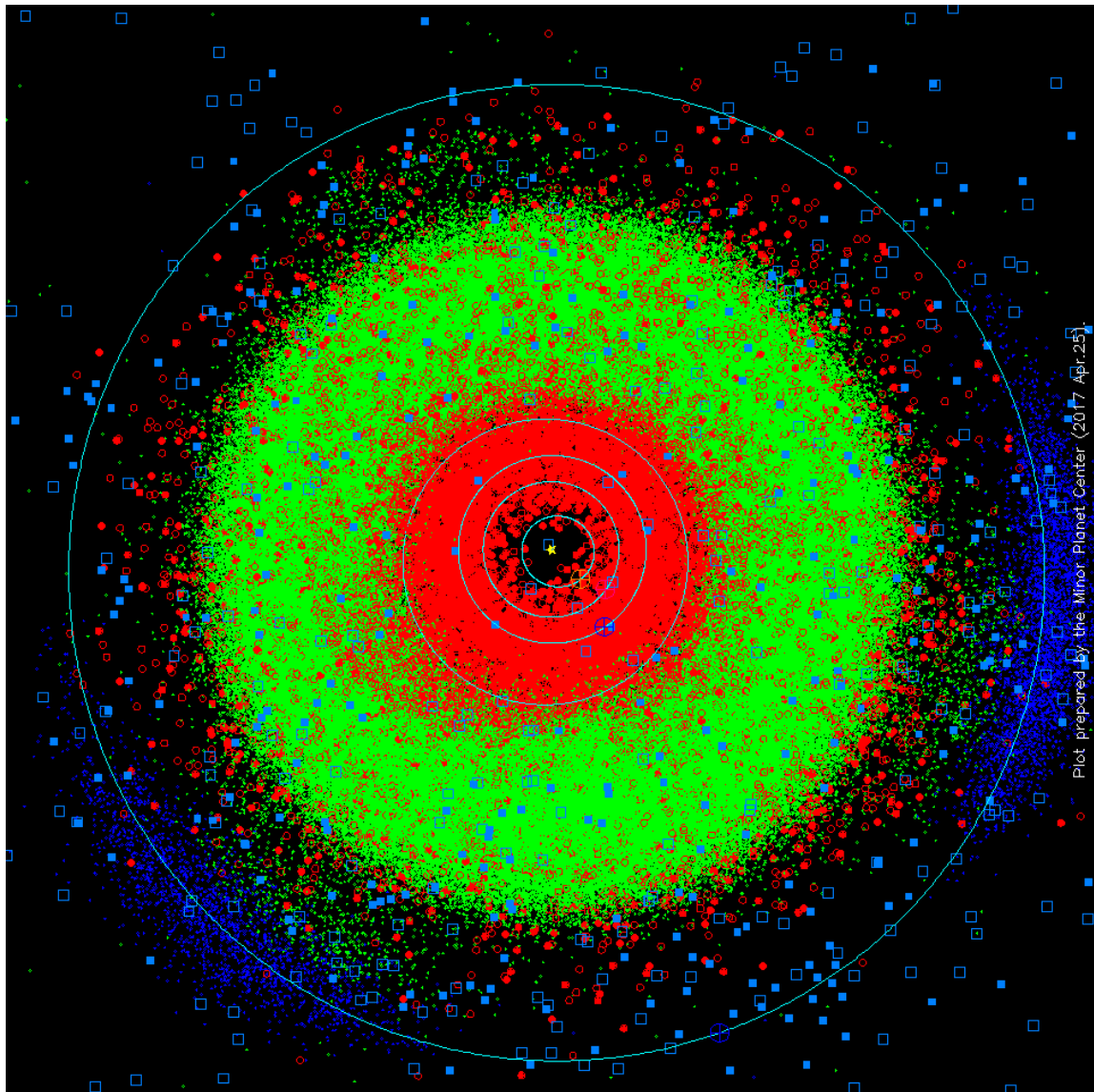
Figure 1. Locations of the minor planets in the Solar System as of 2017 April 25. Most objects in this view orbit in the same direction as Earth, or counterclockwise in this view; the vernal equinox (direction of the Sun as seen from Earth around April 25) is to the right. Solid lines indicate the orbits of the five major planets out to Jupiter (outermost line). Colors of the dots and symbols indicate the population to which they belong. Red solid circles: near-Earth objects observed at multiple oppositions; red open circles: near-Earth objects observed at only one opposition. Dark blue circles: Jupiter Trojans. Light blue squares (solid and open): comets (numbered and unnumbered). Green circles: all other minor planets. Figure courtesy of the Minor Planet Center.
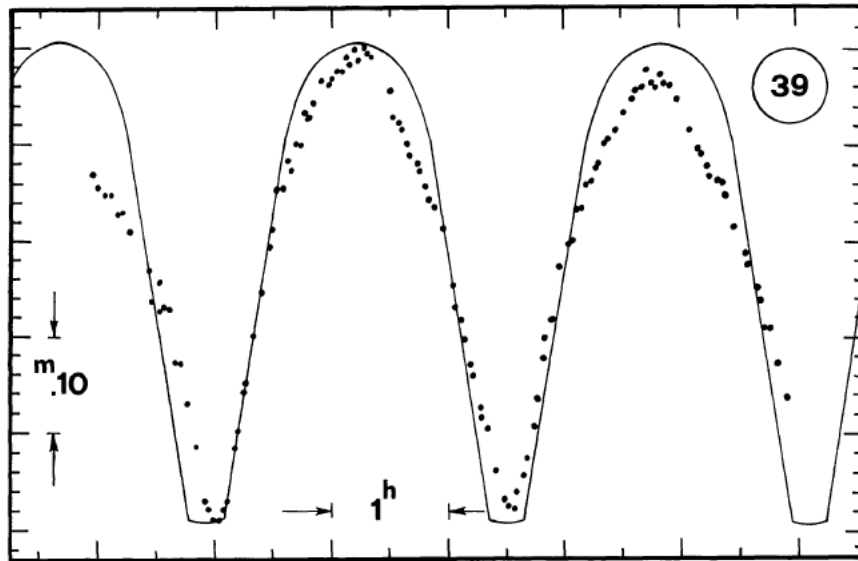
Figure 2. Observed light curve (indicated with dots) of (39) Laetitia from Cellino et al. (1985), overlaid with an "equilibrium binary" model (solid line) from Leone et al. (1984). The vertical axis indicates magnitude, with each large tick mark corresponding to 0.10 mag. The horizontal axis indicates time, with each small tick mark corresponding to half an hour. The flat-bottomed minima and dependency of light on phase angle strongly suggested that this asteroid was part of a binary system.
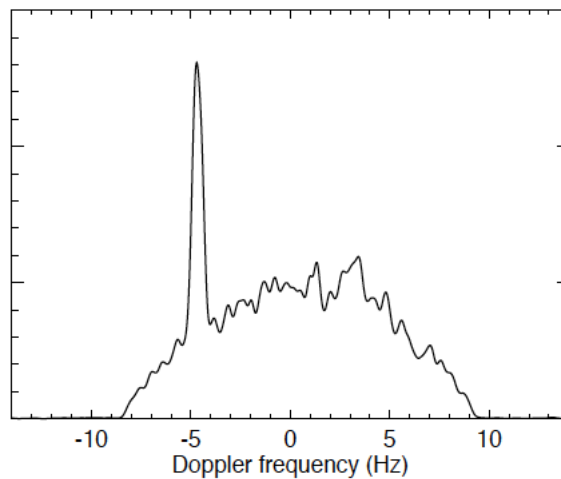
Figure 3. Echo power as a function of Doppler frequency for a binary asteroid. The binarity is evident from the characteristic superimposed peaks: the wider peak represents the fast-rotating primary and the narrow peak is the tidally locked (synchronous) secondary. Figure from Margot et al. (2015).
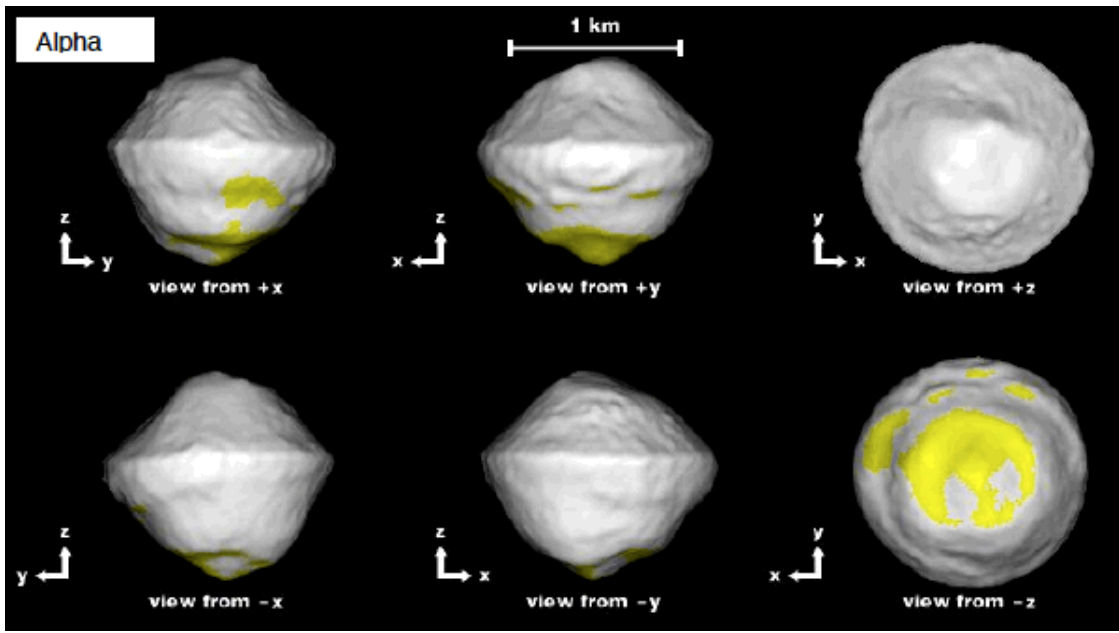
Figure 4. Modeled shape of the primary asteroid in the binary system 1999 KW4 as an example of the distinctive shape resulting from the rotational fission process. Figure adapted from Ostro et al. (2006).
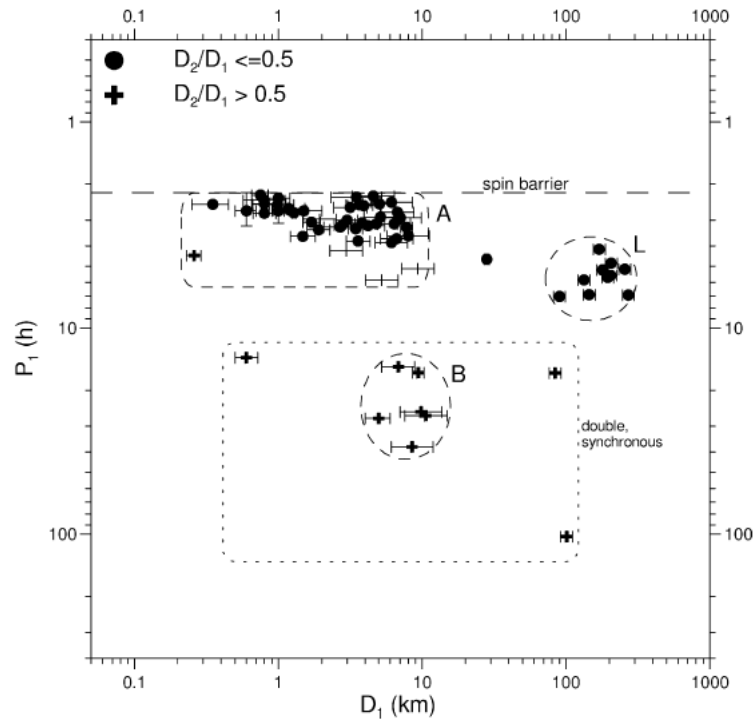
Figure 5. Primary asteroid rotation period (noted here as P_1) and primary asteroid diameter (D_1 here) for asteroids of various size ratios ($D_S/D_P = D_2/D_1$ here). Group A consists of asynchronous binary NEAs and small MBAs and MCs. Group B are synchronous MBAs with components of nearly equal size. Group L systems have large primary asteroids with small companions. Figure from Pravec & Harris (2007).
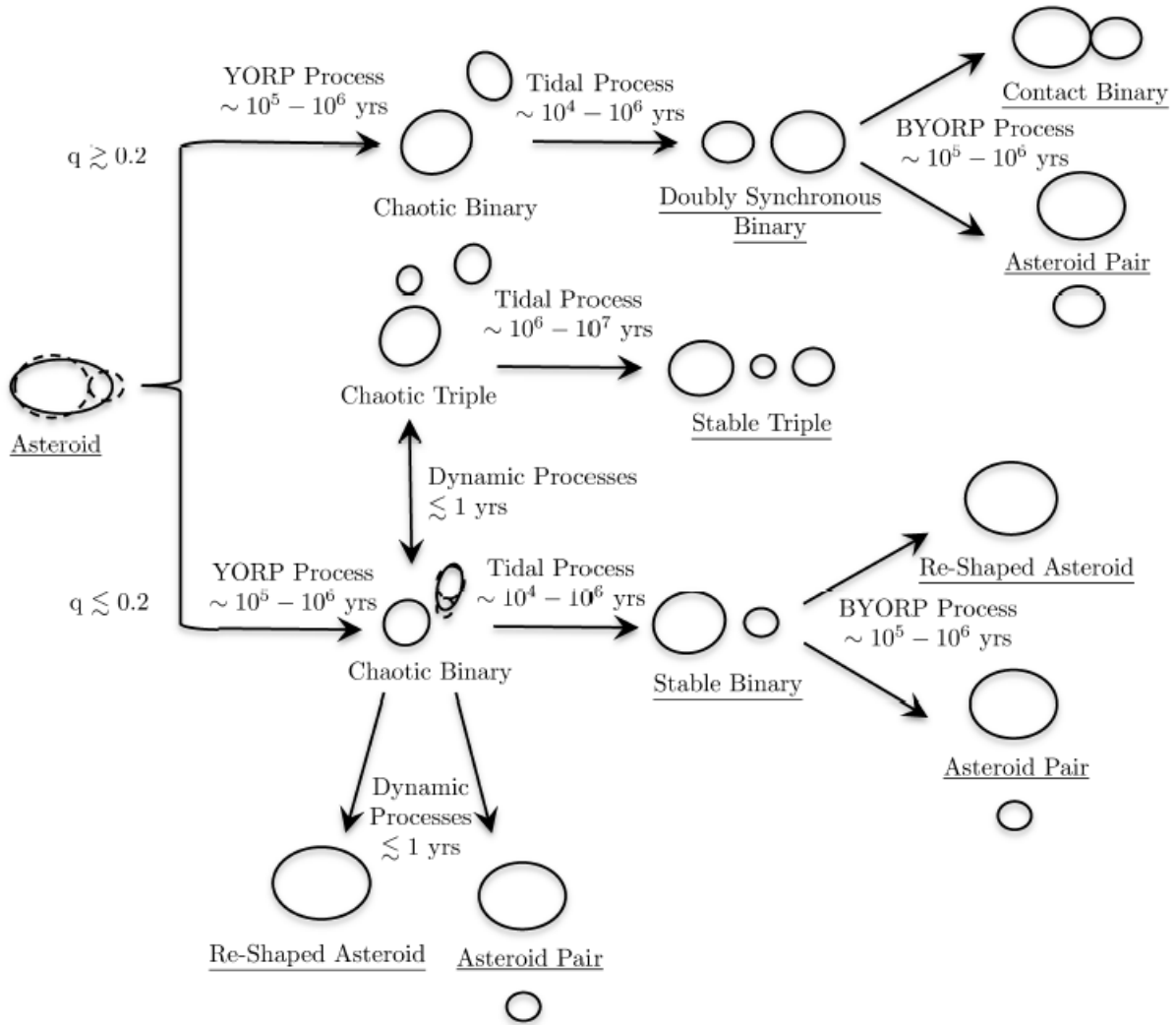
Figure 6. Evolutionary paths for an asteroid experiencing rotational fission. These paths differ critically depending on the mass ratio $q = M_S/M_P$ of the two components, as discussed in Section 5.2. Figure from Jacobson & Scheeres (2011).
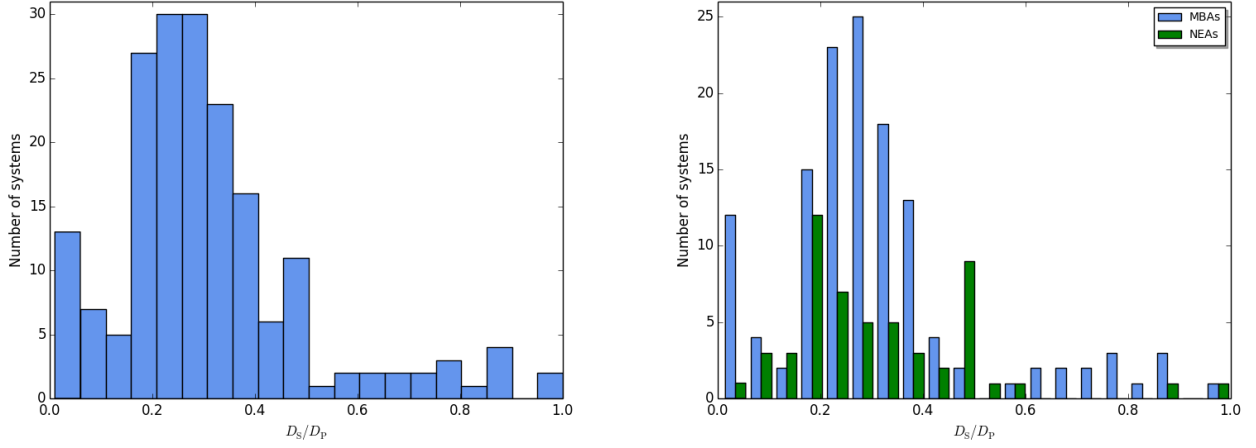
Figure 7. Distributions of size ratios D_S/D_P for NEAs and MBAs. *Left panel:* Distribution for all binary asteroids in these populations combined, separated into 20 equal-width bins. *Right panel:* Distribution for these asteroids separated by their Solar System location and in 20 equal-width bins. Number of systems plotted: 54 NEAs, 133 MBAs. Data are the subset given in Table 1, originally from the compilation by Johnston (2016).
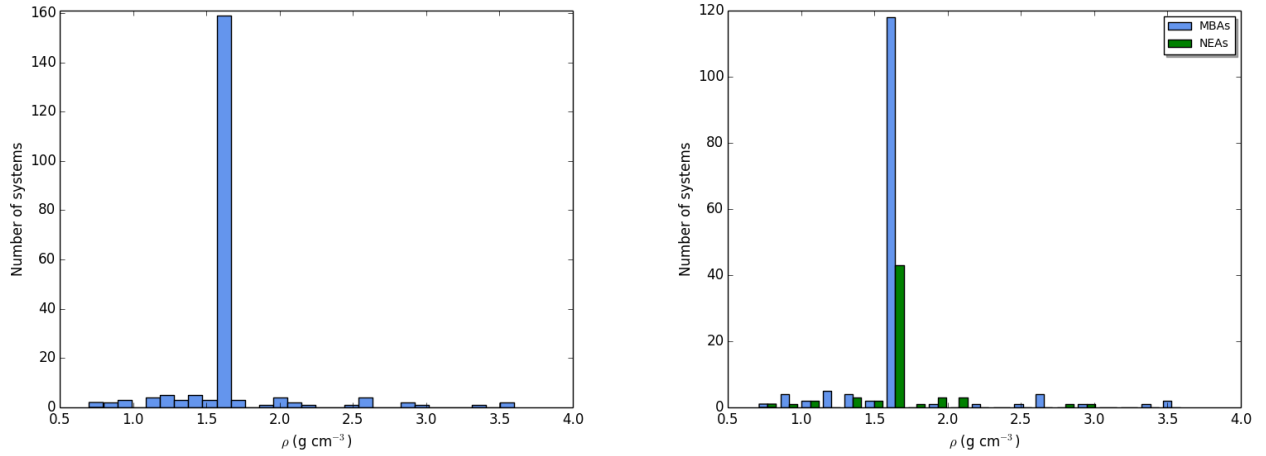
Figure 8. Distributions of density ρ for NEAs and MBAs. *Left panel:* Distribution for all binary asteroids in these populations combined, separated into 30 equal-width bins. *Right panel:* Distribution for these asteroids separated by their Solar System location in 20 equal-width bins. Number of systems plotted: 61 NEAs, 147 MBAs. Data are the subset given in Table 1, originally from the compilation by Johnston (2016).
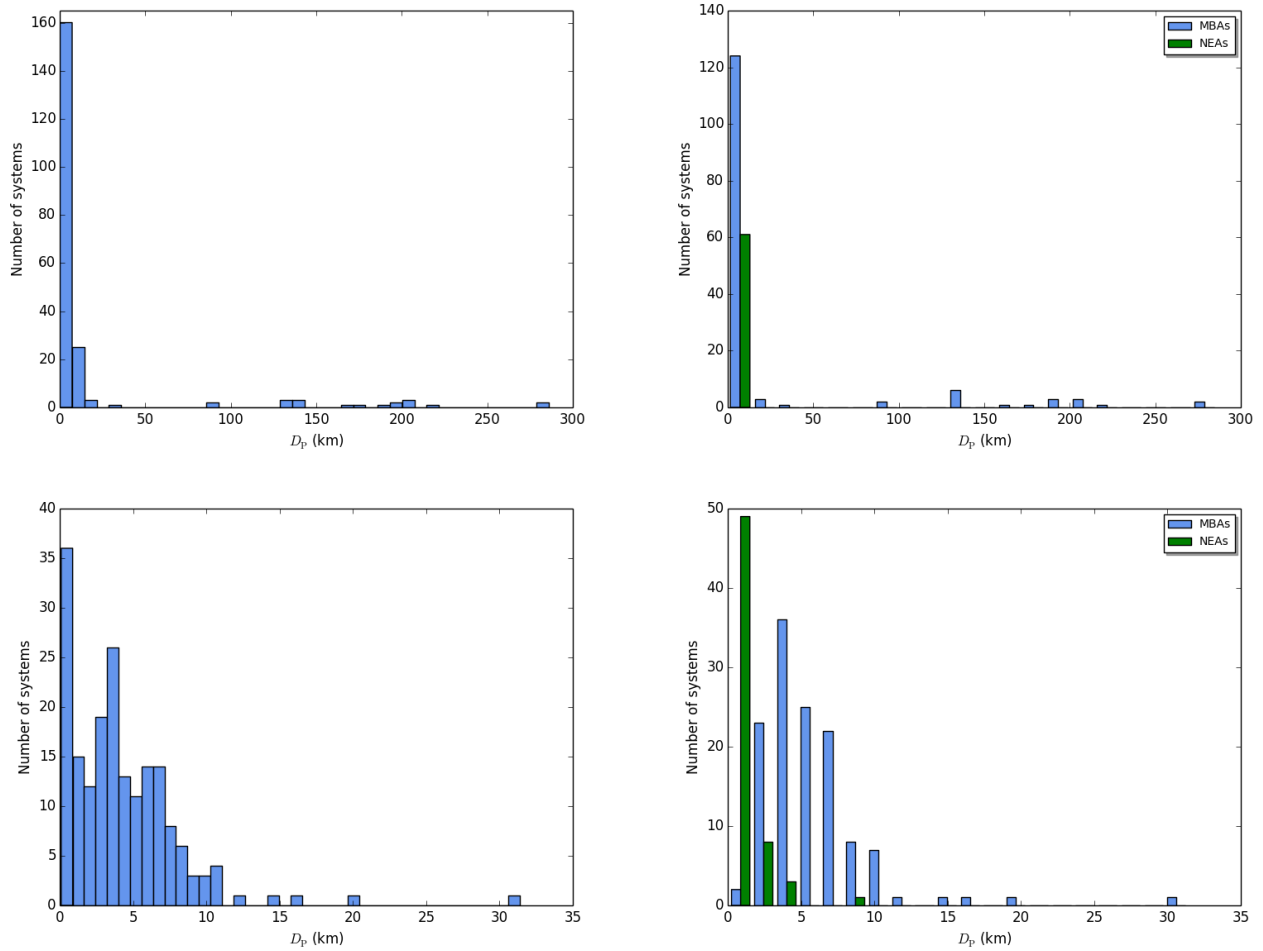
Figure 9. Distributions of primary diameter D_P for NEAs and MBAs. *Left column:* Distributions for all binary asteroids in these populations combined, separated into 40 equal-width bins. *Right column:* Distributions for these asteroids separated by their Solar System location and in 20 equal-width bins. The bottom panels are a re-binning of the systems with diameters less than 50 km. Number of systems plotted: 61 NEAs, 147 MBAs Data are the subset given in Table 1, originally from the compilation by Johnston (2016).
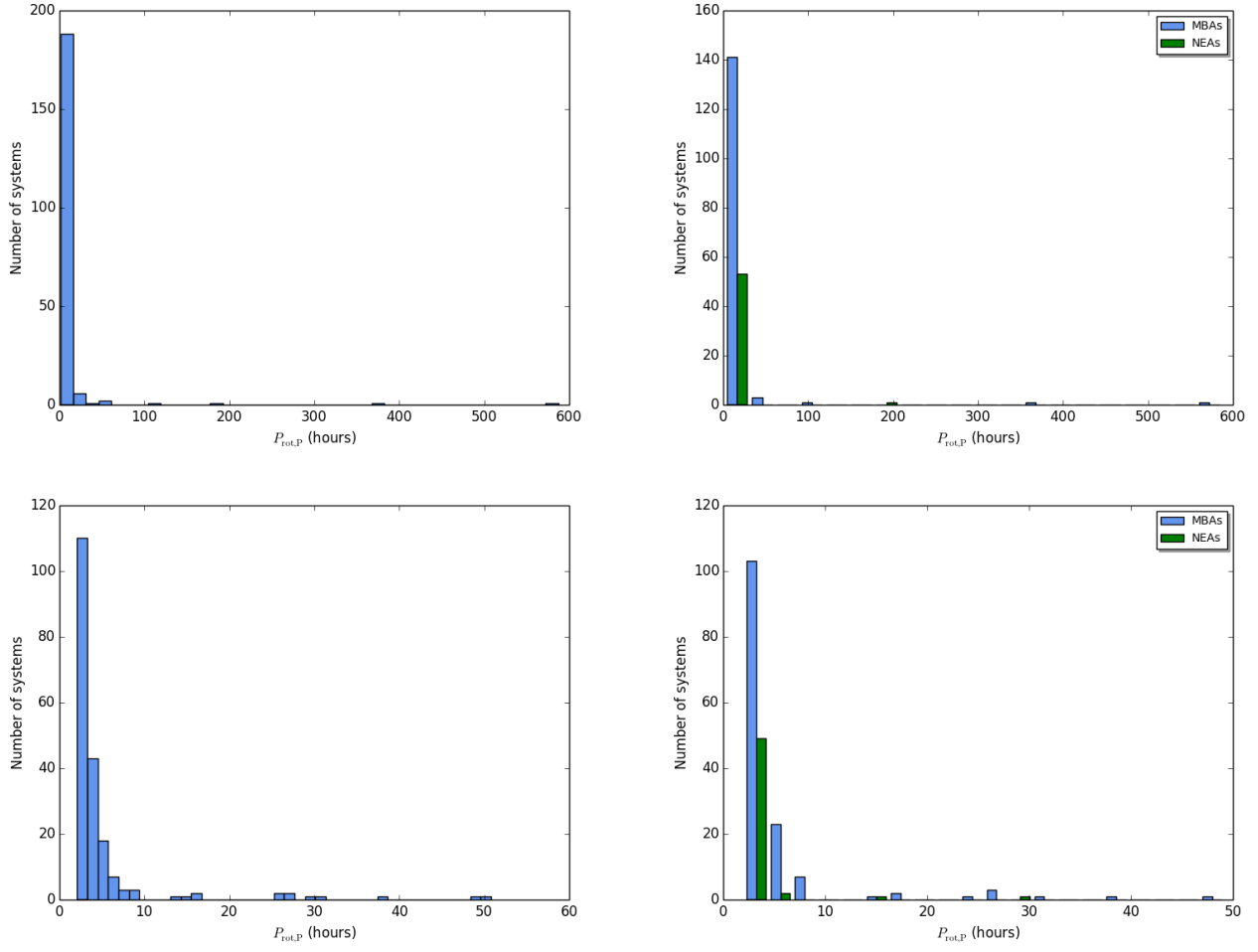
Figure 10. Distributions of primary rotation period $P_{rot,P}$ for NEAs and MBAs. *Left column:* Distributions for all binary asteroids in these populations combined, separated into 40 equal-width bins. *Right column:* Distributions for these asteroids separated by their Solar System location and in 20 equal-width bins. The bottom panels are a re-binning of the systems with rotation periods less than 50 hours. Number of systems plotted: 54 NEAs, 147 MBAs. Data are the subset given in Table 1, originally from the compilation by Johnston (2016).

Table 1. List of near-Earth and Main Belt multi-asteroid systems and selected relevant parameters. Data compiled from the set maintained by Johnston (2016) with non-NEA, non-MBA systems omitted. Error bars are included where available. Parameters not available are marked "N/A." Reference codes are too numerous to list here; they may be found at http://www.astro.gsu.edu/~vrijmoet/asteroidrefs.html.

| System Name	D_S/D_P	ρ (g cm^{-3})	$P_{\mathrm{rot,P}}$ (hours)	D_P (km)	References
(22) Kalliope	0.168 (± 0.012)	3.35 (± 0.33)	4.148	166.2 (± 2.8)	D08a, M90a, D08a
(41) Daphne	0.011	1.95 (± 0.15)	5.988	174.0 (± 11.7)	C08a, T04c, K02a, C08b
(45) Eugenia	0.034 (± 0.01)	1.1 (± 0.1)	5.699	206.14 (± 6.22)	M10a, M11c, M90a, M08d
(87) Sylvia	0.038 (± 0.02)	1.2 (± 0.1)	5.184	286.0 (± 11.0)	F12b, M05a, M90a
(90) Antiope	0.954 (± 0.016)	1.25 (± 0.05)	16.505	87.8 (± 1.0)	D07a
(93) Minerva	0.028 (± 0.014)	1.5 (± 0.2)	5.982 (± 0.001)	141.6 (± 4.0)	M11b, T04c
(107) Camilla	0.073 (± 0.027)	1.4 (± 0.3)	4.844	219.37 (± 5.94)	M08d, M11c, M90a
(121) Hermione	0.171	1.4 (± 0.35)	5.551	187.0 (± 6.0)	D09a
(130) Elektra	0.03 (± 0.008)	1.3 (± 0.3)	5.225	198.93 (± 4.11)	Y16a, M11c, M90a, M08c
(216) Kleopatra	0.066 (± 0.012)	3.6 (± 0.4)	5.385	135.0 (± 5.8)	D11b, D95a
(243) Ida	0.045	2.6 (± 0.5)	4.634	31.4 (± 1.2)	V96a, T96a, B93a, B96a
(283) Emma	0.067 (± 0.037)	0.7 (± 0.2)	6.888 (± 0.007)	134.7 (± 2.35)	M08c, M11c, S78a
(317) Roxane	0.267	1.6	8.169	19.86 (± 0.12)	D10a, M11c, H92a
(379) Huenna	0.066 (± 0.014)	0.85 (± 0.15)	7.022 (± 0.001)	87.47 (± 2.36)	M08c, M11c, H92a
(702) Alauda / 1910 KQ	0.017 (± 0.004)	1.57 (± 0.5)	8.354 (± 0.001)	201.96 (± 4.64)	R11a, M11c, B08b
(762) Pulcova / 1913 SQ	0.134 (± 0.049)	0.9 (± 0.1)	5.839	141.72 (± 1.54)	M08d, M11c, D01a
(809) Lundia / 1915 XP	0.89 (± 0.05)	1.67 (± 0.04)	15.418 (± 0.001)	6.9 (± 2.4)	K09a
(854) Frostia / 1916 S29	0.724	0.89 (± 0.14)	37.728 (± 0.001)	6.35 (± 0.16)	B06a
(939) Isberga / 1920 HR	0.29 (± 0.02)	2.91 (± 1.86)	2.917	12.4 (± 1.8)	C15a
(1052) Belgica / 1925 VD	0.36 (± 0.02)	1.6	2.71	9.79 (± 0.08)	F13c
(1089) Tama / 1927 WB	0.685	2.52 (± 0.3)	16.444 (± 0.001)	10.7 (± 0.5)	B06a
(1139) Atami / 1929 XE	0.833	1.6	27.45	6.0	M06a
(1313) Berna / 1933 QG	0.79	1.22 (± 0.15)	25.464 (± 0.001)	10.6 (± 0.24)	B06a
(1333) Cevenola / 1934 DA	0.35	1.6	4.88 (± 0.02)	16.2	M09a, W02a
(1338) Duponta / 1934 XA	0.23 (± 0.02)	1.6	3.855	7.68 (± 0.06)	G07a
(1453) Fennia / 1938 ED1	0.28 (± 0.02)	1.6	4.412	6.96 (± 0.39)	W08a
(1509) Esclangona / 1938 YG	0.331	1.6	3.253	7.76 (± 0.57)	M03a, W10c
(1717) Arlon / 1954 AC	N/A	1.6	5.148	9.13 (± 0.17)	M11c, C06a
(1727) Mette / 1965 BA	0.21 (± 0.02)	1.6	2.981	10.18	W13h
(1830) Pogson / 1968 HA	0.32	1.6	2.57	7.89 (± 0.11)	H07d
(1862) Apollo / 1932 HA	0.052 (± 0.039)	2.85 (± 0.58)	3.065	1.55 (± 0.07)	O05a, R13a, K07a

Table 1 continued on next page

Table 1 (*continued*)

System Name	D_S/D_P	ρ (g cm^{-3})	$P_{rot,P}$ (hours)	D_P (km)	References
(1866) Sisyphus / 1972 XA	0.1 ($\pm$ 0.05)	1.6	2.401 ($\pm$ 0.001)	8.44 ($\pm$ 1.27)	W16b, D03a, S11b
(2006) Polonskaya / 1973 SB3	0.22	1.6	3.118	4.51 ($\pm$ 0.16)	P05c
(2044) Wirt / 1950 VE	0.25 ($\pm$ 0.02)	1.6	3.69	6.46 ($\pm$ 0.58)	P06f
(2047) Smetana / 1971 UA1	0.21 ($\pm$ 0.02)	1.6	2.497	3.0 ($\pm$ 0.15)	W13c
(2121) Sevastopol / 1971 ME	0.41 ($\pm$ 0.02)	1.6	2.906	8.62 ($\pm$ 0.04)	H10a
(2131) Mayall / 1975 RA	0.3	1.6	2.568	8.2 ($\pm$ 0.07)	P16a, W10c
(2242) Balaton / 1936 TG	0.25	1.6	2.798	5.95	M16a
(2343) Siding Spring / 1979 MD4	0.19	1.6	2.106	5.11	P15a
(2449) Kenos / 1978 GC	N/A	1.6	3.848	6.2	W15b
(2478) Tokai / 1981 JC	0.72	1.6	25.885 ($\pm$ 0.007)	8.1 ($\pm$ 0.02)	H07c
(2486) Metsähovi / 1939 FY	N/A	1.6	4.452	8.42 ($\pm$ 0.03)	M11c, P07a
(2535) Hämeenlinna / 1939 DH	0.22	1.6	3.231	9.2	B16a
(2577) Litva / 1975 EE3	0.35 ($\pm$ 0.02)	1.6	2.813	4.0	W09b, M13a, W11a
(2577) Litva / 1975 EE3	0.3	1.6	2.813	4.0	M13a, W11a
(2623) Zech / A919 SA	0.29	1.6	2.74	7.26	P14a
(2691) Sersic / 1974 KB	0.43 ($\pm$ 0.02)	1.6	3.881	5.0 ($\pm$ 0.11)	O11a
(2754) Efimov / 1966 PD	0.2 ($\pm$ 0.03)	1.6	2.45	6.17	P06c
(2815) Soma / 1982 RL	0.25 ($\pm$ 0.02)	1.6	2.733	6.95 ($\pm$ 0.09)	P11c
(3034) Climenhaga / A917 SE	0.2 ($\pm$ 0.02)	1.6	2.737	9.78	W16b, O13a
(3073) Kursk / 1979 SW11	0.25 ($\pm$ 0.02)	1.6	3.447	6.69	K07c, K07c
(3169) Ostro / 1981 LA	0.87 ($\pm$ 0.01)	2.6 ($\pm$ 0.2)	6.509 ($\pm$ 0.001)	3.89 ($\pm$ 0.06)	D07b
(3309) Brorfelde / 1982 BH	0.26 ($\pm$ 0.02)	1.6	2.504	4.88 ($\pm$ 0.08)	W05d
(3433) Fehrenbach / 1963 TJ1	0.31	1.6	3.916	7.4	P15d
(3671) Dionysus / 1984 KD	0.2 ($\pm$ 0.02)	1.6 ($\pm$ 0.65)	2.705	1.43 ($\pm$ 0.2)	P06b
(3673) Levy / 1985 QS	0.28 ($\pm$ 0.03)	1.6	2.688 ($\pm$ 0.001)	6.17 ($\pm$ 0.15)	P07e
(3703) Volkonskaya / 1978 PU3	0.4	1.6	3.235	3.46 ($\pm$ 0.1)	P06b
(3749) Balam / 1982 BG1	0.466	2.6	2.805	3.95	M08a, M08c
(3749) Balam / 1982 BG1	0.42 ($\pm$ 0.03)	2.6	2.805	3.95	P11b, M08a, M08c
(3782) Celle / 1986 TE	0.43 ($\pm$ 0.01)	2.2 ($\pm$ 0.4)	3.839 ($\pm$ 0.002)	5.44 ($\pm$ 0.21)	R04a
(3841) Dicicco / 1983 VG7	0.28	1.6	3.595	6.02	F14b
(3868) Mendoza / 4575 P-L	0.22 ($\pm$ 0.02)	1.6	2.771	9.13 ($\pm$ 0.05)	O09a
(3873) Roddy / 1984 WB	0.27 ($\pm$ 0.02)	1.6	2.48	7.25 ($\pm$ 0.24)	W12a
(3905) Doppler / 1984 QO	0.77	1.6	50.8 ($\pm$ 0.1)	6.27	F13b, H14a
(3951) Zichichi / 1986 CK1	0.33	1.6	3.394	6.38 ($\pm$ 0.2)	A11a
(3982) Kastel / 1984 JP1	N/A	1.6	8.849	6.79 ($\pm$ 0.36)	M11c, W15d
(4029) Bridges / 1982 KC1	0.24 ($\pm$ 0.02)	1.6	3.575	7.8 ($\pm$ 0.07)	H06d
(4272) Entsuji / 1977 EG5	0.18	1.6	2.809	7.56	B15b
(4383) Suruga / 1989 XP	0.21 ($\pm$ 0.02)	1.6	3.407	6.33 ($\pm$ 0.09)	W13d
(4440) Tchantches / 1984 YV	0.25 ($\pm$ 0.03)	1.6	2.788	2.03 ($\pm$ 0.57)	W13d
(4492) Debussy / 1988 SH	0.643	0.91 ($\pm$ 0.1)	26.606 ($\pm$ 0.001)	14.6 ($\pm$ 0.59)	B06a
(4514) Vilen / 1972 HX	0.26	1.6	2.892	6.09	P15e
(4541) Mizuno / 1989 AF	0.24	1.6	2.828	6.12 ($\pm$ 1.3)	P15f

Table 1 (*continued*)

System Name	D_S/D_P	ρ (g cm^{-3})	$P_{\mathrm{rot,P}}$ (hours)	D_P (km)	References
(4607) Seilandfarm / 1987 WR	0.29	1.6	3.968	7.1 ($\pm$ 0.12)	P09b
(4666) Dietz / 1986 JA1	N/A	1.6	2.952	6.83 ($\pm$ 0.29)	P16b
(4674) Pauling / 1989 JC	0.316	1.6	2.521	4.46 ($\pm$ 0.05)	M04b, P11b
(4765) Wasserburg / 1986 JN1	0.16 ($\pm$ 0.02)	1.6	3.623 ($\pm$ 0.001)	1.76 ($\pm$ 0.48)	W13i
(4786) Tatianina / 1985 PE2	0.19 ($\pm$ 0.03)	1.6	2.923	3.22 ($\pm$ 0.2)	P06d
(4868) Knushevia / 1989 UN2	0.13 ($\pm$ 0.03)	1.6	3.142	1.52 ($\pm$ 0.32)	W15e
(4951) Iwamoto / 1990 BM	0.76	1.6	118.0 ($\pm$ 0.2)	4.39 ($\pm$ 0.02)	R07b
(5143) Heracles / 1991 VL	0.167 ($\pm$ 0.1)	1.6	2.706 ($\pm$ 0.001)	3.6 ($\pm$ 1.2)	T12b, P12a
(5381) Sekhmet / 1991 JY	0.3 ($\pm$ 0.052)	1.98 ($\pm$ 0.65)	2.7 ($\pm$ 0.4)	1.0 ($\pm$ 0.05)	N03a
(5407) 1992 AX	0.2 ($\pm$ 0.02)	1.6	2.549	3.9 ($\pm$ 1.0)	P06b
(5425) Vojtech / 1984 SA1	0.22 ($\pm$ 0.02)	1.6	2.648	6.89 ($\pm$ 0.13)	S15b
(5426) Sharp / 1985 DD	N/A	1.6	4.561	2.03 ($\pm$ 0.34)	W15g
(5474) Gingasen / 1988 XE1	0.7 ($\pm$ 0.2)	1.6	3.624	4.14 ($\pm$ 0.55)	W16b, H08a
(5477) Holmes / 1989 UH2	0.37 ($\pm$ 0.02)	1.6	2.994	2.95 ($\pm$ 0.13)	W05a
(5481) Kiuchi / 1990 CH	0.33 ($\pm$ 0.02)	1.6	3.62	6.86	K08b
(5646) 1990 TR	0.18 ($\pm$ 0.02)	1.6	3.2	2.68 ($\pm$ 0.51)	W13c
(5899) Jedicke / 1986 AH	0.32	1.6	2.748 ($\pm$ 0.001)	2.54 ($\pm$ 0.16)	W10b, W13a
(5905) Johnson / 1989 CJ1	0.4 ($\pm$ 0.04)	1.6	3.782	4.45 ($\pm$ 0.07)	W05b, W05b
(6084) Bascom / 1985 CT	0.37 ($\pm$ 0.02)	1.6	2.745	5.96 ($\pm$ 0.21)	H06c
(6244) Okamoto / 1990 QF	0.25 ($\pm$ 0.02)	1.6	2.896	6.39	H06a, H06a
(6265) 1985 TW3	0.24 ($\pm$ 0.02)	1.6	2.709	4.81 ($\pm$ 0.1)	H07b
(6369) 1983 UC	0.36 ($\pm$ 0.02)	1.6	2.397	4.86 ($\pm$ 1.17)	W16b
(6615) Plutarchos / 9512 P-L	0.26 ($\pm$ 0.03)	1.6	2.325	3.04 ($\pm$ 0.04)	W16b, M11c, O07a
(6708) Bobbievaile / 1989 AA5	0.57	1.6	8.221 ($\pm$ 0.002)	8.02 ($\pm$ 0.02)	P09a
(7088) Ishtar / 1992 AA	0.42 ($\pm$ 0.02)	1.6	2.679	1.39	R06c
(7187) Isobe / 1992 BW	0.16 ($\pm$ 0.03)	1.6	4.243	5.97 ($\pm$ 1.44)	W16b
(7225) Huntress / 1983 BH	0.21 ($\pm$ 0.02)	1.6	2.44	6.54 ($\pm$ 0.22)	P08c
(7369) Gavrilin / 1975 AN	0.32	1.6	49.12 ($\pm$ 0.02)	5.23 ($\pm$ 1.34)	H08a
(7888) 1993 UC	N/A	1.6	2.34	2.72	P96a
(7958) Leakey / 1994 LE3	0.3 ($\pm$ 0.03)	1.6	2.348	2.82 ($\pm$ 0.16)	W12c
(8026) Johnmckay / 1991 JA1	N/A	1.6	372.0 ($\pm$ 5.0)	1.69 ($\pm$ 0.24)	M11c, W11a
(8116) Jeanperrin / 1987 WU3	0.33	1.6	3.617	4.53 ($\pm$ 0.08)	H07a
(8306) Shoko / 1995 DY1	0.4	1.6	3.35	3.06	P13a
(8373) Stephengould / 1992 AB	0.27	1.6	4.435	5.29	K10b
(8474) Rettig / 1985 GA1	0.86	1.6	30.54 ($\pm$ 0.01)	4.5	C15b
(9069) Hovland / 1993 OV	0.3	1.6	4.218	3.0	W05b
(9260) Edwardolson / 1953 TA1	0.27 ($\pm$ 0.03)	1.6	3.085	3.98 ($\pm$ 0.35)	J05a
(9617) Grahamchapman / 1993 FA5	0.27 ($\pm$ 0.03)	1.6	2.286	2.74 ($\pm$ 0.37)	P06e
(9783) Tensho-kan / 1994 YD1	0.26 ($\pm$ 0.04)	1.6	3.011	5.16 ($\pm$ 0.27)	W16b
(10123) Fideoja / 1993 FJ16	0.36 ($\pm$ 0.02)	1.6	2.866	3.27 ($\pm$ 0.49)	W16b
(10208) Germanicus / 1997 QN1	0.46 ($\pm$ 0.02)	1.6	3.348	3.23 ($\pm$ 0.18)	O07b
(11217) 1999 JC4	N/A	1.6	4.822	3.3	W14a

Table 1 continued on next page

Table 1 (*continued*)

System Name	D_S/D_P	ρ (g cm^{-3})	$P_{rot,P}$ (hours)	D_P (km)	References
(11264) Claudiomaccone / 1979 UC4	0.31	1.2	3.187 ($\pm$ 0.001)	4.0	K07b
(13123) Tyson / 1994 KA	N/A	1.6	3.33	10.87 ($\pm$ 2.26)	W16b
(15268) Wendelinefroger / 1990 WF3	0.27	1.6	2.422	3.83	O08a
(15430) 1998 UR31	N/A	1.6	2.527	3.74 ($\pm$ 0.03)	M11c, O13a
(15700) 1987 QD	0.31 ($\pm$ 0.03)	1.6	3.059	3.62	W16b, D10b
(15822) 1994 TV15	0.19 ($\pm$ 0.02)	1.6	2.96	1.69 ($\pm$ 0.3)	W14a
(16525) Shumarinaiko / 1991 CU2	0.16 ($\pm$ 0.02)	1.6	2.593	5.18 ($\pm$ 0.15)	W13e
(16635) 1993 QO	0.35	1.6	2.208	4.5	P16a
(17246) 2000 GL74	0.222	1.6	5.0	4.5	D10a P11b
(17260) 2000 JQ58	0.26 ($\pm$ 0.03)	1.6	3.129	4.41	H06b
(18890) 2000 EV26	0.27 ($\pm$ 0.02)	1.6	3.822 ($\pm$ 0.001)	2.07 ($\pm$ 0.19)	W15a
(20325) 1998 HO27	0.3 ($\pm$ 0.02)	1.6	3.245	4.73 ($\pm$ 0.97)	W16b, M11c, P14b
(21436) Chaoyichi / 1998 FL116	0.35 ($\pm$ 0.02)	1.6	2.865	1.84 ($\pm$ 0.25)	W16b
(22899) 1999 TO14	0.222	1.6	4.03 ($\pm$ 0.03)	5.54 ($\pm$ 0.46)	D10a, P11b
(26074) Carlwirtz / 1977 TD	N/A	1.6	2.459	3.46	W13a
(26416) 1999 XM84	0.27 ($\pm$ 0.02)	1.6	2.966	4.4	W16b
(26471) 2000 AS152	0.36 ($\pm$ 0.02)	1.6	2.687	5.69 ($\pm$ 0.41)	W10c
(27568) 2000 PT6	N/A	1.6	3.488	1.82 ($\pm$ 0.42)	M11c, W13g
(31345) 1998 PG	0.3	1.6	2.516	0.9 ($\pm$ 0.2)	P06b, P00a
(31450) 1999 CU9	0.22	1.6	3.412	10.4	P15g
(32008) 2000 HM53	0.4	1.6	3.017	4.04	P07b
(32039) 2000 JO23	0.65 ($\pm$ 0.07)	1.6	6.598 ($\pm$ 0.001)	3.33	W16b, P07d
(34706) 2001 OP83	0.28 ($\pm$ 0.02)	1.6	2.594	3.48	W06a
(35107) 1991 VH	0.4 ($\pm$ 0.02)	1.6 ($\pm$ 0.5)	2.624	1.04 ($\pm$ 0.2)	P06b, P06b, P06b
(43008) 1999 UD31	0.4 ($\pm$ 0.05)	1.6	2.742	2.32	W16b
(44620) 1999 RS43	0.34 ($\pm$ 0.02)	1.6	3.14	2.46	W16b, P16a
(46829) 1998 OS14	0.4 ($\pm$ 0.02)	1.6	2.624	3.06	P15c
(51356) 2000 RY76	0.21 ($\pm$ 0.02)	1.6	2.557	3.23	W13
(52316) 1992 BD	0.16 ($\pm$ 0.02)	1.6	2.763	3.26	W13c
(53110) 1999 AR7	0.41 ($\pm$ 0.02)	1.6	2.738 ($\pm$ 0.001)	1.4	W16a
(53432) 1999 UT55	0.23 ($\pm$ 0.02)	1.6	3.33 ($\pm$ 0.002)	2.55	W13d
(65803) Didymos / 1996 GT	0.22 ($\pm$ 0.02)	1.7 ($\pm$ 0.4)	2.259	0.75 ($\pm$ 0.1)	P06b
(66063) 1998 RO1	0.48 ($\pm$ 0.03)	1.5 ($\pm$ 1.15)	2.492	0.8 ($\pm$ 0.15)	P06b, S09a
(66391) 1999 KW4	0.341 ($\pm$ 0.025)	1.97 ($\pm$ 0.24)	2.765	1.32 ($\pm$ 0.04)	O06a
(69230) Hermes / 1937 UB	0.9 ($\pm$ 0.09)	1.6	13.894 ($\pm$ 0.004)	0.6 ($\pm$ 0.12)	P06b
(69406) 1995 SX48	0.19 ($\pm$ 0.02)	1.6	4.486 ($\pm$ 0.001)	3.12 ($\pm$ 0.02)	W14b
(76818) 2000 RG79	0.37 ($\pm$ 0.03)	1.6	3.166	3.6	P06b, W05c
(79472) 1998 AX4	0.32 ($\pm$ 0.03)	1.6	2.88	3.61	W12b
(80218) 1999 VO123	0.32 ($\pm$ 0.02)	1.6	3.145	1.52	P16a
(85938) 1999 DJ4	0.5 ($\pm$ 0.05)	1.6	2.514	0.43 ($\pm$ 0.08)	P06b, P06b, K10a
(88710) 2001 SL9	0.28 ($\pm$ 0.02)	1.6	2.4	0.96	P06b
(99913) 1997 CZ5	0.19 ($\pm$ 0.02)	1.6	2.835	6.77	H11b

Table 1 continued on next page

Table 1 (*continued*)

System Name	D_S/D_P	ρ (g cm^{-3})	$P_{\mathrm{rot,P}}$ (hours)	D_P (km)	References
(114319) 2002 XD58	N/A	1.6	7.954	2.62	P05b
(136617) 1994 CC	0.182 ($\pm$ 0.052)	2.1 ($\pm$ 0.6)	2.389	0.62 ($\pm$ 0.06)	B11a
(136617) 1994 CC	0.129 ($\pm$ 0.05)	2.1 ($\pm$ 0.6)	2.389	0.62 ($\pm$ 0.06)	B11a
(136993) 1998 ST49	0.109 ($\pm$ 0.056)	1.6	2.302 ($\pm$ 0.001)	0.69 ($\pm$ 0.08)	W14c
(137170) 1999 HF1	0.23 ($\pm$ 0.03)	2.0	2.319	3.64 ($\pm$ 0.73)	P06b, P02a
(138095) 2000 DK79	N/A	1.6	4.243 ($\pm$ 0.001)	2.18	W14e
(153591) 2001 SN263	0.308 ($\pm$ 0.061)	1.13 ($\pm$ 0.15)	3.426	2.5 ($\pm$ 0.3)	B15a
(153591) 2001 SN263	0.172 ($\pm$ 0.06)	1.13 ($\pm$ 0.15)	3.426	2.5 ($\pm$ 0.3)	B15a
(153958) 2002 AM31	0.25	3.0	2.817	0.45 ($\pm$ 0.05)	T13a, W14c
(162000) 1990 OS	0.167 ($\pm$ 0.068)	1.6	2.536	0.3 ($\pm$ 0.02)	O03b, O03b, B03a
(162483) 2000 PJ5	0.5	1.6	2.642 ($\pm$ 0.001)	0.55	P08b
(164121) 2003 YT1	0.191 ($\pm$ 0.065)	2.01 ($\pm$ 0.7)	2.343	1.1 ($\pm$ 0.2)	N04a, P06b, B06c
(175706) 1996 FG3	0.28 ($\pm$ 0.015)	1.3 ($\pm$ 0.5)	3.595	1.63 ($\pm$ 0.04)	S09a, Y14a, P16a, S15a
(185851) 2000 DP107	0.366 ($\pm$ 0.029)	1.38 ($\pm$ 0.24)	2.774 ($\pm$ 0.001)	0.86 ($\pm$ 0.04)	N15c
(190208) 2006 AQ	N/A	1.6	182.0 ($\pm$ 2.0)	0.79	W15c
(218144) 2002 RL66	N/A	1.6	587.0 ($\pm$ 10.0)	3.3	W10d
(276049) 2002 CE26	0.087 ($\pm$ 0.03)	0.9 ($\pm$ 0.45)	3.293	3.46 ($\pm$ 0.35)	S06a
(285263) 1998 QE2	0.25 ($\pm$ 0.034)	0.7 ($\pm$ 0.2)	4.751 ($\pm$ 0.001)	3.2 ($\pm$ 0.3)	S14a, H14b
(311066) 2004 DC	0.2	1.73 ($\pm$ 0.49)	2.6	0.36	T08a, C12a
(348400) 2005 JF21	0.5	1.6	N/A	0.6	N15a
(357439) 2004 BL86	0.21 ($\pm$ 0.02)	1.6	2.62	0.3	P15b
(363027) 1998 ST27	0.15	1.6	3.0	0.8	B03b
(363067) 2000 CO101	0.065	1.6	5.12 ($\pm$ 0.01)	0.62	J10a, W10a
(363599) 2004 FG11	0.533	1.6	4.0	0.15 ($\pm$ 0.03)	T12a, B14e
(374851) 2006 VV2	0.167	1.6	2.41 ($\pm$ 0.005)	1.8	B07a, B08b
(385186) 1994 AW1	0.49 ($\pm$ 0.02)	1.4 ($\pm$ 0.5)	2.519	0.9 ($\pm$ 0.09)	P06b, R15a
(399307) 1991 RJ2	0.47 ($\pm$ 0.02)	1.6	3.491	0.5	W15f
(399774) 2005 NB7	0.32	1.6	3.488	0.5 ($\pm$ 0.11)	S08a, K08a
(410777) 2009 FD	0.6	1.6	4.0	0.15 ($\pm$ 0.03)	N15b, N15b
(450894) 2008 BT18	0.333	1.6	2.726 ($\pm$ 0.007)	0.6	B08c, B09a
(452561) 2005 AB	0.24 ($\pm$ 0.02)	1.6	3.339 ($\pm$ 0.002)	1.9	R06b, R06b, R06b
(461852) 2006 GY2	0.2	1.6	2.27 ($\pm$ 0.01)	0.4	B06b, H08b
1994 CJ1	1.0	1.6	30.0	0.15	B14d, T14a, W14d
1994 XD	0.25	1.6	2.736 ($\pm$ 0.001)	0.6 ($\pm$ 0.15)	B05a, W13c
2000 UG11	0.5 ($\pm$ 0.09)	1.47 ($\pm$ 0.7)	4.44 ($\pm$ 0.01)	0.26 ($\pm$ 0.03)	P06b, M02b
2002 BM26	0.167 ($\pm$ 0.051)	1.6	2.7	0.6 ($\pm$ 0.03)	N02a
2002 KK8	0.2 ($\pm$ 0.041)	1.6	N/A	0.5 ($\pm$ 0.02)	N02b, N02b
2003 SS84	0.5 ($\pm$ 0.186)	1.6	N/A	0.12 ($\pm$ 0.02)	N03b
2005 YQ96	N/A	1.6	N/A	0.27	
2007 DT103	0.267	1.6	2.703 ($\pm$ 0.04)	0.3	B07b, A09a
2007 LE	0.36	1.6	2.603 ($\pm$ 0.005)	0.5	B12a,, H12a
2008 DG17	N/A	1.6	N/A	0.38	

Table 1 (*continued*)

System Name	D_S/D_P	ρ (g cm^{-3})	$P_{rot,P}$ (hours)	D_P (km)	References
2013 WT44	N/A	1.6	2.885	1.0 ($\pm$ 0.1)	B14c, W14d
2014 WZ120	0.32 ($\pm$ 0.02)	1.6	3.361 ($\pm$ 0.002)	0.26	W15c
2014 YB35	0.5	1.6	N/A	0.3	N15d
2015 TD144	N/A	1.6	N/A	0.1	

REFERENCES

Becker, T., Howell, E. S., Nolan, M. C., & Magri, C. 2008, Bulletin of the American Astronomical Society, 40, 28.06

Belton, M. J. S., Veverka, J., Thomas, P., et al. 1992, Science, 257, 1647

Belton, M. J. S., Chapman, C. R., Thomas, P. C., et al. 1995, Nature, 374, 785

Bottke, W. F., & Melosh, H. J. 1996, Nature, 381, 51

Bottke, W. F., Jr., Vokrouhlický, D., Rubincam, D. P., & Broz, M. 2002, Asteroids III, 395

Cellino, A., Pannunzio, R., Zappala, V., Farinella, P., & Paolicchi, P. 1985, A&A, 144, 355

Chapman, C. R., Veverka, J., Thomas, P. C., et al. 1995, Nature, 374, 783

Chauvineau, B., & Mignard, F. 1990, Icarus, 87, 377

Ćuk, M., & Burns, J. A. 2005, Icarus, 176, 418

Davis, D. R., Chapman, C. R., Weidenschilling, S. J., & Greenberg, R. 1985, Icarus, 62, 30

Delbo, M., Walsh, K., Mueller, M., Harris, A. W., & Howell, E. S. 2011, Icarus, 212, 138

Descamps, P., Marchis, F., Michalowski, T., et al. 2007, Icarus, 187, 482

Descamps, P., Marchis, F., Michalowski, T., et al. 2009, Icarus, 203, 102

Durda, D. D. 1996, Icarus, 120, 212

Durda, D. D., Bottke, W. F., Enke, B. L., et al. 2004, Icarus, 170, 243

Gehrels, T., Drummond, J. D., & Levenson, N. A. 1987, Icarus, 70, 257

Gradie, J., & Flynn, L. 1988, Lunar and Planetary Science Conference, 19,

Jacobson, S. A., & Scheeres, D. J. 2011, Icarus, 214, 161

Johnston, W. R. 2016, NASA Planetary Data System, 244,

Leone, G., Paolicchi, P., Farinella, P., & Zappala, V. 1984, A&A, 140, 265

Margot, J. L., & Brown, M. E. 2001, Bulletin of the American Astronomical Society, 33, 52.02

Margot, J. L., Nolan, M. C., Benner, L. A. M., et al. 2002, Science, 296, 1445

Margot, J.-L., Pravec, P., Taylor, P., Carry, B., & Jacobson, S. 2015, Asteroids IV, 355

Melosh, H. J., & Stansberry, J. A. 1991, Icarus, 94, 171

Merline, W. J., Chapman, C. R., Robinson, M., et al. 1998, Lunar and Planetary Science Conference, 29,

Merline, W. J., Close, L. M., Dumas, C., et al. 1999, IAUC, 7129, 1

Merline, W. J., Close, L. M., Dumas, C., et al. 1999, Nature, 401, 565

Merline, W. J., Chapman, C. R., Colwell, W. B., et al. 1999, Lunar and Planetary Science Conference, 30,

Merline, W. J., Close, L. M., Shelton, J. C., et al. 2000, IAUC, 7503, 3

Merline, W. J., Close, L. M., Dumas, C., et al. 2000, Bulletin of the American Astronomical Society, 32, 13.06

Merline, W. J., Close, L. M., Menard, F., et al. 2001, Bulletin of the American Astronomical Society, 33, 52.01

Merline, W. J., Weidenschilling, S. J., Durda, D. D., et al. 2002, Asteroids III, 289

Merline, W. J., Close, L. M., Siegler, N., et al. 2002, IAUC, 7827, 2

Merline, W. J., Tamblyn, P. M., Dumas, C., et al. 2002, IAUC, 7980, 2

Nolan, M. C., Howell, E. S., Becker, T. M., et al. 2008, Bulletin of the American Astronomical Society, 40, 25.04

Ostro, S. J., Margot, J.-L., Benner, L. A. M., et al. 2006, Science, 314, 1276

Petit, J.-M., & Mousis, O. 2004, Icarus, 168, 409

Polishook, D., & Brosch, N. 2009, Icarus, 199, 319

Pravec, P., & Hahn, G. 1997, Icarus, 127, 431

Pravec, P., & Harris, A. W. 2000, Icarus, 148, 12

Pravec, P., Scheirich, P., Kušnirák, P., et al. 2006, Icarus, 181, 63

Pravec, P., & Harris, A. W. 2007, Icarus, 190, 250

Pravec, P., Harris, A. W., Vokrouhlický, D., et al. 2008, Icarus, 197, 497

Pravec, P., Vokrouhlický, D., Polishook, D., et al. 2010, Nature, 466, 1085

Richardson, D. C., & Walsh, K. J. 2006, Annual Review of Earth and Planetary Sciences, 34, 47

Rossi, A., Marzari, F., & Scheeres, D. J. 2009, Icarus, 202, 95

Rubincam, D. P. 2000, Icarus, 148, 2

Stokes, G. H., Evans, J. B., Viggh, H. E. M., Shelly, F. C., & Pearce, E. C. 2000, Icarus, 148, 21

Storrs, A., Wells, E., Zellner, B., Stern, A., & Durda, D. 1999, AAS/Division for Planetary Sciences Meeting Abstracts #31, 31, 11.03

Veverka, J., Thomas, P. C., Bell, J. F., III, et al. 1999, Science, 285, 562

Vokrouhlický, D., Bottke, W. F., Chesley, S. R., Scheeres, D. J., & Statler, T. S. 2015, Asteroids IV, 509

Walsh, K. J., & Jacobson, S. A. 2015, Asteroids IV, 375

Warner, B. D., Harris, A. W., & Pravec, P. 2009, Icarus, 202, 134

Weidenschilling, S. J. 1980, BAAS, 12, 662

Weidenschilling, S. J. 1980, Icarus, 44, 807